Chinese Chemical Letters 31 (2020) 2891–2896

Contents lists available at ScienceDirect

Chinese Chemical Letters

journal homepage: www.elsevier.com/locate/cclet

Communication

The regulation of biothiol-responsive performance and bioimaging application of benzo[*c*][1,2,5]oxadiazole dyes

Dongyang Li[a], Weijie Chen[a], Sheng Hua Liu[a], Xiaoqiang Chen[b], Jun Yin[a,b,*]

[a] *Key Laboratory of Pesticide and Chemical Biology, Ministry of Education, Hubei International Scientific and Technological Cooperation Base of Pesticide and Green Synthesis, International Joint Research Center for Intelligent Biosensing Technology and Health, College of Chemistry, Central China Normal University, Wuhan 430079, China*

[b] *State Key Laboratory of Materials-Oriented Chemical Engineering, College of Chemical Engineering, Jiangsu National Synergetic Innovation Center for Advanced Materials (SICAM), Nanjing Tech University, Nanjing 211816, China*

ARTICLE INFO

Article history:
Received 27 December 2019
Received in revised form 21 February 2020
Accepted 24 February 2020
Available online 4 March 2020

Keywords:
Benzo[*c*][1,2,5]oxadiazole dye
Sulfoxide
Sulphone
Thiol response

ABSTRACT

The different oxidation states of sulphur atom play a significant role on functional materials. In this work, a aryl-thioether and its sulphone substituted benzo[*c*][1,2,5]oxadiazole dyes were synthesized and utilized to determine thiol-containing amino acids. The result of selectivity experiments showed they detected the cysteine and homocysteine under physiological condition with negligible interference from other amino acids. In comparison to the thioether dye, the sulphone-based dye exhibited much faster response time for Cys and Hcy. However, the sulphone restricted its thiol-reactivity and bioimaging performance in living cells. By reducing the oxidation state of sulphur atom, we amazedly found that the sulfoxide-based dye still maintained high selectivity ultrafast response time for Cys/Hcy under physiological condition. It was worth mentioning that it also had high reactivity and good bioimaging performance that sulfone compounds did not have.

Thiol-containing amino acids, *e.g.*, cysteine (Cys), homocysteine (Hcy) and glutathione (GSH), play significant role in maintaining redox homeostasis in biological systems [1]. Abnormal alterations of their concentrations considered to be signals of various pathogenesis and dysfunction in living systems are closely associated with many human diseases such as AIDS, Alzheimer's, as well as cancer, liver damage, growth retardation and cardiovascular diseases [2]. Accordingly, numerous efforts have been paid to the development of simple and effective methods to rapidly track biothiols in biological systems. Recently, fluorescence probes and bioimaging technology [3] have made great achievements in development of biothiol-responsive fluorescent probes due to its excellent sensitivity, high selectivity and excellent biocompatibility [4,5].

In our group, we have developed a type of thiol-specific fluorescent probes by employing the naphthalimide as fluorophore and sulfonamide as the detecting group to track the thiol level in living cells, tissues and *in vivo* [6]. However, these probes exhibited a relatively slow response time. To promote the response rate of fluorescent probes, some new detecting groups was reported constantly. For instance, the thioether-type detecting group involving the mechanism of nucleophilic substitution was installed on all kinds of fluorophores to construct the thiol-responsive fluorescent probes by some groups [7,8]. Based on the mechanism of nucleophilic substitution of these thiol-responsive fluorescent probes, varying the oxidation state of sulphur atom would possibly change the activity of nucleophilic substitution [9]. Accordingly, in this work, we proposed an effective oxidation strategy to synthesize thiol-responsive benzo[*c*][1,2,5]oxadiazole dyes containing sulphur atom with different oxidation state, and investigated the effect of the oxidation state of sulphur atom on thiol-responsive rate and their bioimaging application.

Dyes NBD-S and NBD-SO_2 were obtained according to the synthetic route in Fig. 1A. Firstly, thiophenol was treated with the commercially available 4-chloro-7-nitrobenzo[*c*][1,2,5]thiadiazole (NBD-Cl) to yield the targeting thioether (NBD-S). Subsequent oxidation produced the sulphone-based dye (NBD-SO_2). Their structures have been well characterized by ^{1}HNMR, ^{13}C NMR and mass spectroscopies (Supporting information). In particular, their single crystals suitable for crystallographic analysis were obtained

* Corresponding author at: Key Laboratory of Pesticide and Chemical Biology, Ministry of Education, Hubei International Scientific and Technological Cooperation Base of Pesticide and Green Synthesis, International Joint Research Center for Intelligent Biosensing Technology and Health, College of Chemistry, Central China Normal University, Wuhan 430079, China.
E-mail address: yinj@mail.ccnu.edu.cn (J. Yin).

https://doi.org/10.1016/j.cclet.2020.02.047
1001-8417/

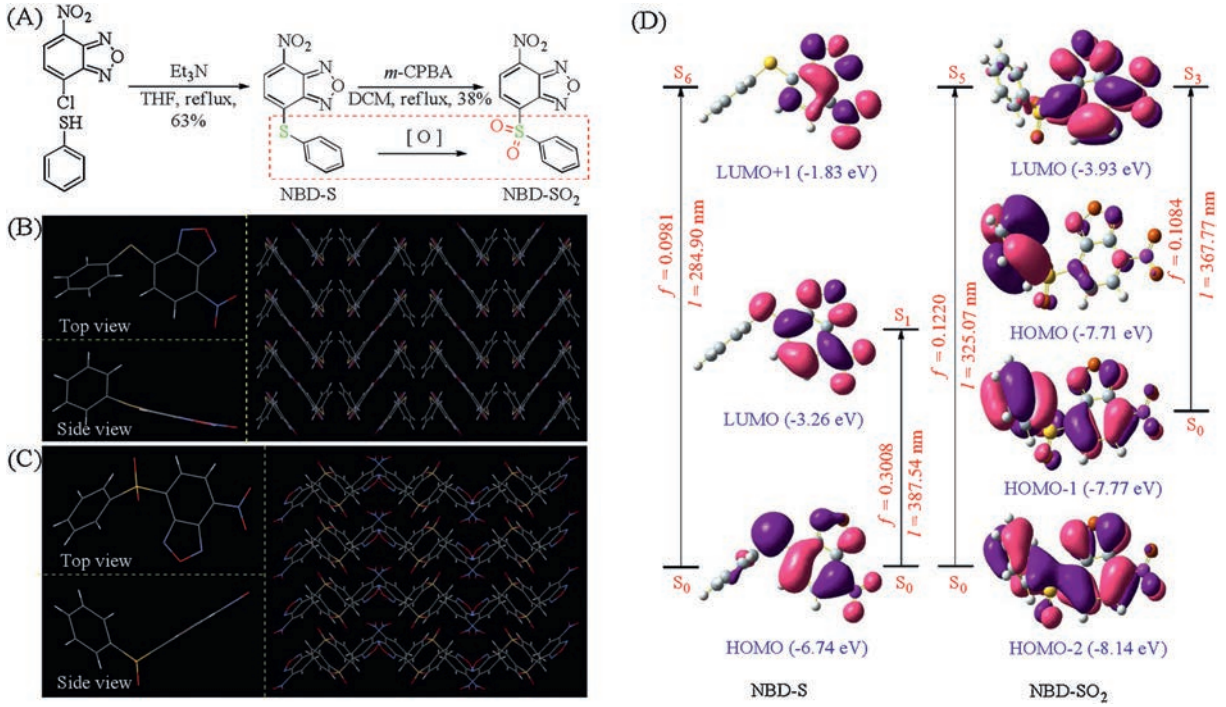

Fig. 1. (A) The synthetic of dyes NBD-S and NBD-SO_2. (B) The crystal structure of NBD-S. (C) The crystal structure of NBD-SO_2. (D) The frontier molecular orbital profiles of NBD-S and NBD-SO_2 based on TD-DFT (B3LYP/6-31G*) calculations.

by slow diffusion of hexane into a THF solution of NBD-S and a CH_2Cl_2 solution of NBD-SO_2 at room temperature, respectively. From the crystral structure of NBD-S in Fig. 1B, there were multiple weak intermolecular interactions including C—H···O, C—H···S, C—H···N and $\pi\cdots\pi$ interactions while NBD-SO_2 in Fig. 1C mainly involved in two weak interactions including C—H···O and C—H$\cdots\pi$ interaction (Tables S1-S3, Figs. S1 and S2 in Supporting information). These multiple interactions led to the highly ordered stacking in crystalline phases.

To assess the electronic properties of dyes, time-dependent density functional theory (TD-DFT) calculations were carried out at the B3LYP/6-31G* level with the Gaussian 09 program to investigate their frontier molecular orbitals and electronic transitions. In Fig. 1D, the electron density of HOMO and LUMO of NBD-S predominantly assigned to NBD moiety. Two intense transitions were predicted at about 388 nm with a larger oscillator strength of 0.3008 (HOMO → LUMO) and 285 nm with a larger oscillator strength of 0.0918 (HOMO → LUMO + 1), implying that dye NBD-S had weak fluorescence for weak charge transfer (Table S4 in Supporting information). For dye NBD-SO_2, the HOMO orbital was predominantly assigned to the phenylsulphone unit while the LUMO orbital was mainly located the NBD moiety, and there are two intense transitions with a larger oscillator strength of 0.1220 (HOMO-2 → LUMO) and 0.1084 (HOMO-1 → LUMO) at 325 nm and 368 nm, respectively. The result suggested that NBD-SO_2 was non-fluorescent probably due to a process of electron transfer.

In view of the sensitivity of thioether group towards biothiols, their UV–vis absorption and fluorescent spectra were explored in HEPES buffer solution (10 mmol/L, pH 7.4) containing 1% DMSO to evaluate the selectivity of dyes NBD-S and NBD-SO_2. In UV–vis absorption spectra (Fig. S3 in Supporting information), dyes NBD-S and NBD-SO_2 showed similar absorption changes from 426 nm to 480 nm upon addition of Cys and Hcy, respectively. In fluorescence spectra, the blank solution of dyes NBD-S and NBD-SO_2 were almost non-fluorescent, which were well in agreement with the result of above theoretical calculation. However, remarkable fluorescence enhancements at 550 nm were found upon the addition of Cys and Hcy, respectively, as shown in Figs. 2A and B, while other amino acids including GSH only induced negligible fluorescence changes. And according to the changes of fluorescence intensity, it was found that the reaction equilibrium of dye

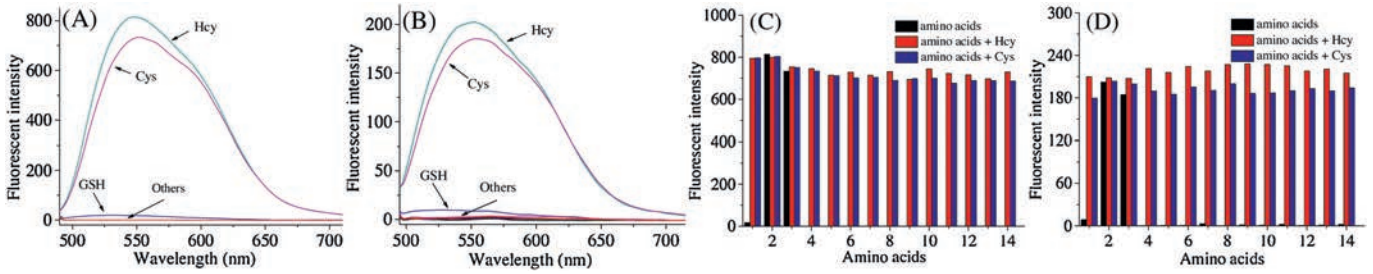

Fig. 2. Fluorescence changes of dyes NBD-S (A) and NBD-SO_2 (B) (10 μmol/L) upon the addition of Cys, Hcy and other various analytes (100 μmol/L) in HEPES buffer solution (10 mmol/L, pH 7.4) containing 1% DMSO. Florescence intensity changes at 550 nm of dyes NBD-S (C) and NBD-SO_2 (D) (10 μmol/L) toward Cys (blue bars) and Hcy (red bars) in the presence of various analytes (100 μmol/L). Analytes 1-14: (1) GSH, (2) Hcy, (3) Cys, (4) D-Glu, (5) Ala, (6) Tyr, (7) Lys, (8) L-Glu, (9) Ser, (10) His, (11) Arg, (12) Met, (13) Gln, (14) Phe. λ_{ex} = 475 nm and slit width of 11 nm × 9 nm.

NBD-SO_2 was lower than dye NBD-S probably as a result of inferior reactivity with Cys/Hcy. This observation was consistent with previous report [9]. Subsequently, the further fluorescence competitive assays were performed to assess the interferences from other analytes. The results in Figs. 2C and D indicated that Cys and Hcy still induced distinct fluorescence changes of dyes NBD-S and NBD-SO_2 in the presence of other amino acids, strongly suggesting that dyes NBD-S and NBD-SO_2 had high specificity towards Cys/Hcy with little interferences from other similar analytes. For the sensing mechanism, we supposed that the spectra changes were caused by the addition of Cys/Hcy through the nucleophilic substitution reaction to produce the fluorescent substituted products [10], which were confirmed by ESI mass spectrometry (Fig. S4 in Supporting information).

Next, their sensing capability for Cys/Hcy with different concentrations in HEPES buffer solution (10 mmol/L, pH 7.4) containing 1% DMSO was investigated. In UV–vis absorption spectra, the main absorption peak of dye NBD-S at 428 nm gradually decreased and a new peak at 484 nm emerged concurrently with a well-defined isosbestic point at 438 nm upon the addition of Cys/Hcy (Fig. S5 in Supporting information). And the corresponding fluorescence intensity at 550 nm showed a gradual enhancement along with the addition of Cys/Hcy (Figs. 3A and B). It was worth mentioning that the fluorescence intensity changes were linearly proportional to the Cys/Hcy concentration (Fig. S6 in Supporting information). According to the formula of $3\sigma/k$ [11], the detection limits of dye NBD-S were 9.7×10^{-8} mol/L for Cys, and 9.4×10^{-8} mol/L for Hcy, respectively. These observations indicated that NBD-S could serve as a promising means for detecting Cys/Hcy quantitatively.

Then, the time-dependent response of dyes NBD-S and NBD-SO_2 (10 μmol/L) towards Cys, Hcy and GSH (100 μmol/L) were tested in HEPES buffer solution (10 mmol/L, pH 7.4) containing 1% DMSO. As shown in Fig. 3C, the fluorescent intensity of dye NBD-S at 550 nm gradually increased to its maximum around within 50 min for Cys and Hcy while GSH did not follow such significance fluorescence change (Figs. S7A-C in Supporting information). As comparison, its oxidation sulphone-based dye NBD-SO_2 responding Cys or Hcy to reach the maximum was around within 1 min and 15 min in Fig. 3D (Figs. S7D-F in Supporting information), respectively. The result suggested that the different oxidation state of leaving group sulphur had a large influence on the response time of biothiols.

In our previous work, we found that the different pH environment had a large effect for the biothiols responsibility [7e]. Therefore, their responsibility in HEPES buffer solution (10 mmol/L) containing 1% DMSO at various pH values was studied. The fluorescence spectra revealed that the optimal conditions for dyes NBD-S (Fig. S8A in Supporting information) to detect Cys/Hcy was around pH 7.0, indicating that the dye might be suitable to monitor biothiols under physiological conditions. In comparison to the dye NBD-S, the responsibility of dye NBD-SO_2 toward biothiols was significantly improved under same condition, and it could selectively detect Cys at pH 5.0 (Figs. S8B, S9 and S10 in Supporting information).

The above investigation *in vitro* confirmed that dyes NBD-S and NBD-SO_2 could be used to visualize the level of Cys/Hcy in living cells. Accordingly, the cytotoxicity of dyes was investigated by CCK-8 assay. The result suggested that dye NBD-S (Fig. S11A in Supporting information) had low cytotoxicity. For the dye NBD-SO_2, it also exhibited low cytotoxicity partially due to its poor cell permeability (Fig. S11B in Supporting information). Subsequently, dyes NBD-S and NBD-SO_2 were utilized to monitor intracellular Cys and Hcy. As could be observed by viewing Fig. 4, a quite strong fluorescence signal (Fig. 4B) was found in HeLa cells when they were incubated with dye NBD-S (5 μmol/L) for 30 min, indicating that dye NBD-S was capable of permeating into cells and perceiving the existence of endogenous Cys and Hcy. Moreover, it was further verified by the subsequent control experiments. The HeLa cells pre-treated with the biothiol-blocking reagent NEM (1 mmol/L) for 30 min and then incubated with dye NBD-S for 30 min didn't show fluorescence signal in Fig. 4C. As expected, the addition of Cys in Fig. 4D and Hcy in Fig. 4E (100 μmol/L) to the HeLa cells pre-treated by NEM induced a significant fluorescence, while no obvious change was detected upon the addition of GSH in Fig. 4F. These results indicated that NBD-S can be used to mark the Cys/Hcy in living cells. For the sulphone NBD-SO_2, the bioimaging experiments showed that NBD-SO_2 had poor cell permeability in comparison to the dye NBD-S (Figs. S11B and S12 in Supporting information).

According to the above investigation, dye NBD-SO_2 with higher oxidation state of sulphur atom had faster responsive rate than NBD-S, however NBD-S exhibited high reactivity for Cys/Hcy and better cell membrane permeability. The reported literature indicated that the sulfoxide group had a good reactivity with sulfhydryl groups [9]. Accordingly, we guessed justifiably that the sulphur atom of sulfoxide structure was in the intermediate valence of thioether and sulphone structures, and the NBD dye with sulfoxide group would probably have good thiol-reactivity and cell membrane permeability as well as NBD-S. Moreover, it possibly had fast responsive time like NBD-SO_2. Based on the consideration, dye NBD-SO was synthesized subsequently by oxidizing NBD-S under the condition of less equivalent oxidant and lower temperature, as shown in Fig. 5A. Its structure was also well-confirmed by ^{1}H NMR, ^{13}C NMR and mass spectroscopies (Figs. S30-S32 in Supporting information). Furthermore, we also obtained its single crystals by slow diffusion of hexane into a CH_2Cl_2 solution of NBD-SO at room temperature. The crystallographic analysis (Fig. 5B, Tables S5 and S6 in Supporting information) verified the sulphoxide structure, and the stacking involved in multiple weak intermolecular interactions, *e.g.*, C—H···O, C—H···π interactions (Fig. S13 in Supporting

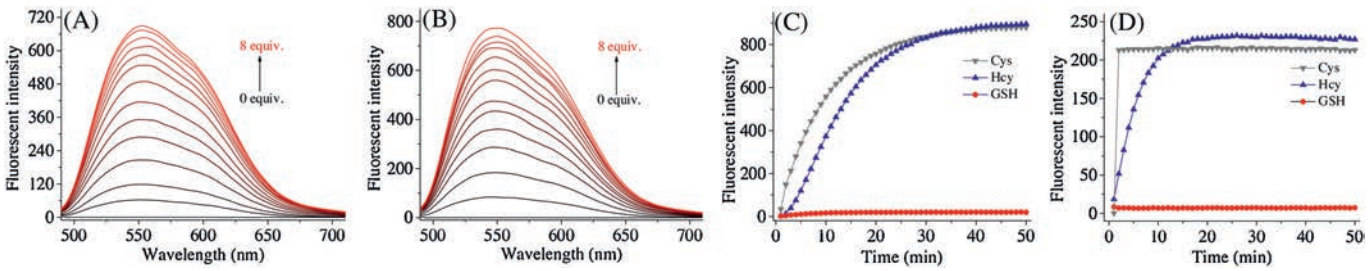

Fig. 3. Fluorescence spectra of dye NBD-S upon the gradual addition of Cys (A) or Hcy (B) (0–8 equiv.) in HEPES buffer solution (10 mmol/L, pH 7.4) containing 1% DMSO. The time-dependent fluorescence intensity changes at 550 nm of dyes NBD-S (C) and NBD-SO_2 (D) (10 μmol/L) with Cys, Hcy or GSH (100 μmol/L) in HEPES buffer solution (10 mmol/L, pH 7.4) containing 1% DMSO. λ_{ex} = 475 nm and slit width of 11 nm × 9 nm.

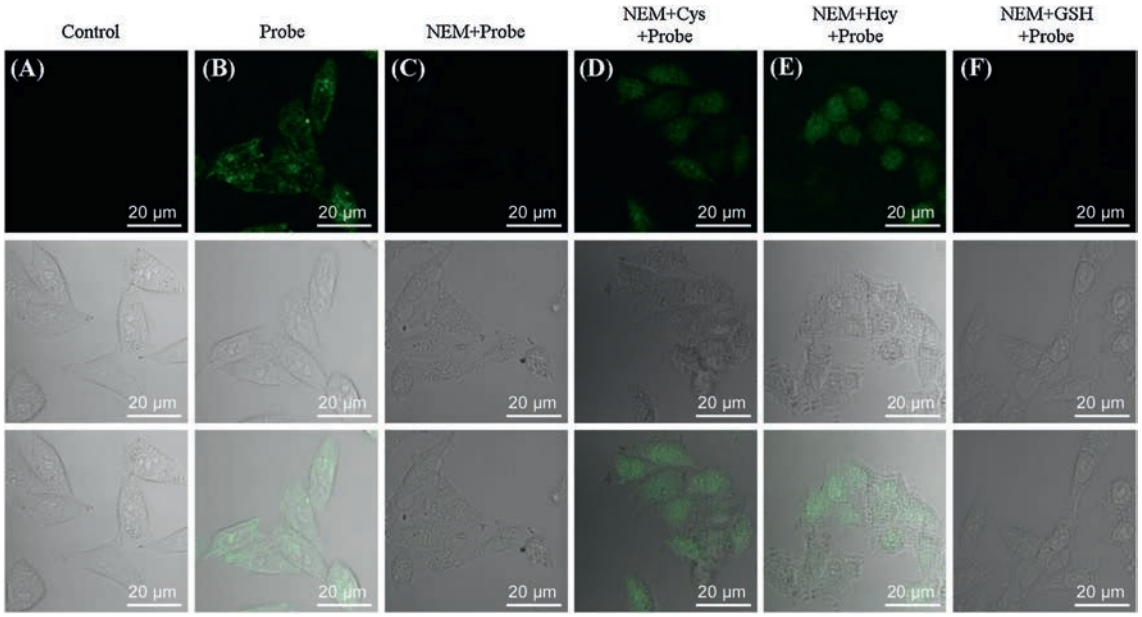

Fig. 4. Confocal microscope images of dye NBD-S responding to biothiols in HeLa cells. (A) Fluorescence images of HeLa cells as control. (B) Fluorescence images of HeLa cells incubated with dye NBD-S (5 μmol/L) for 30 min. (C) Fluorescence images of HeLa cells pre-treated with NEM (1 mmol/L) for 30 min, and incubated with dye NBD-S (5 μmol/L) for 30 min. (D-F) Fluorescence images of HeLa cells pre-treated with NEM (1 mmol/L, 30 min), then treated with Cys (D), Hcy (E) or GSH (F) (100 μmol/L, 30 min), and then incubated with dye NBD-S (5 μmol/L, 30 min). (Top) Images of green channel. (Middle) Images of bright field. (Bottom) Overlay of bright field and green channel.

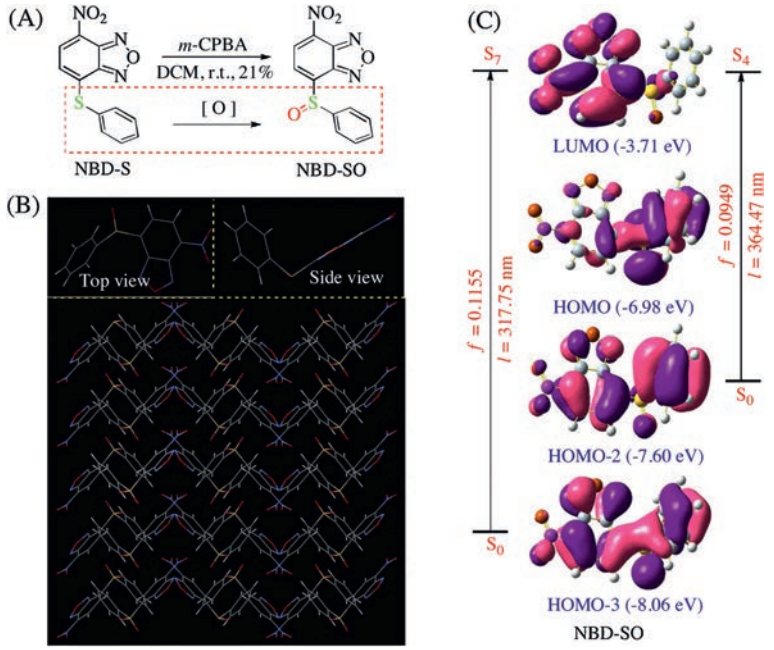

Fig. 5. (A) The synthetic of dye NBD-SO. (B) The single crystal structure of NBD-SO. (C) The frontier molecular orbital profiles of NBD-SO based on TD-DFT (B3LYP/6-31G*) calculations.

information). To gain insight into the electronic properties of NBD-SO, the similar TD-DFT calculation was carried out. From the frontier molecular orbitals containing the main electronic transitions in Fig. 5C, there was an analogous electronic distribution as NBD-SO_2. The electron density of HOMO orbital was predominantly distributed to the aryl-sulphoxide group whereas the electron density of the LUMO orbital mainly assigned to NBD component. More, there were two main absorption bands belong to S_0-S_4 transition at around 364 nm demonstrated a larger oscillator strength of 0.0949 corresponding to 57% contribution from the HOMO-2 to LUMO, and S_0-S_7 transition at around 318 nm demonstrated a large oscillator strength of 0.1155 corresponding to 68% contribution from the HOMO-3 to LUMO, implying that dye NBD-SO involved in a process of electron transfer.

For dye NBD-SO, we firstly investigated its selectivity towards various biothiols. In UV–vis absorption spectra (Fig. S14 in Supporting information), it was found that addition of Cys and Hcy induced a new similar absorption at 480 nm, respectively. Furthermore, obvious fluorescence changes at 550 nm in HEPES buffer solution (10 mmol/L, pH 7.4) containing 1% DMSO were observed when only Cys and Hcy were added to its buffer solution in Fig. 6A. And the competitive experiment further indicated that

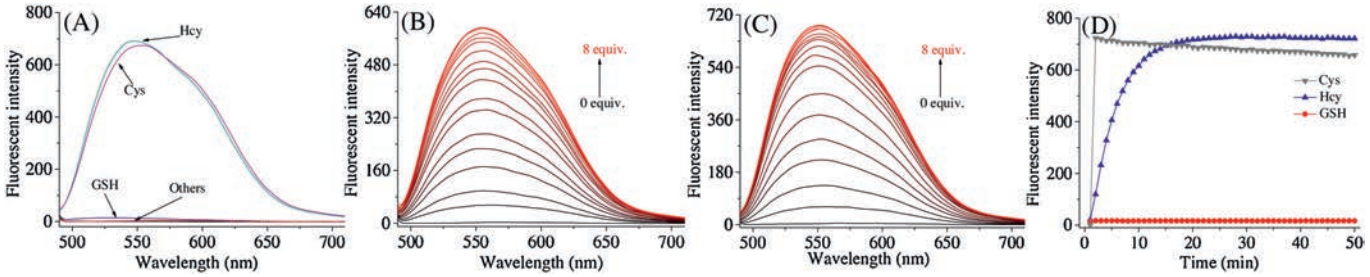

Fig. 6. (A) Fluorescent spectra of dye NBD-SO (10 μmol/L) upon the addition of Cys, Hcy and other various analytes (100 μmol/L) in HEPES buffer solution (10 mmol/L, pH 7.4) containing 1% DMSO. λ_{ex} = 475 nm and slit width of 11 nm × 9 nm. (B) Fluorescence spectra of dye NBD-SO upon the gradual addition of Cys (0-8 equiv.) in HEPES buffer solution (10 mmol/L, pH 7.4) containing 1% DMSO. λ_{ex} = 475 nm and slit width of 11 nm × 9 nm. (C) Fluorescence spectra of dye NBD-SO upon the gradual addition of Hcy (0-8 equiv.) in HEPES buffer solution (10 mmol/L, pH 7.4) containing 1% DMSO. λ_{ex} = 475 nm and slit width of 11 nm × 9 nm. (D) The time-dependent fluorescence intensity changes at 550 nm of dye NBD-SO (10 μmol/L) with Cys, Hcy or GSH (100 μmol/L) in HEPES buffer solution (10 mmol/L, pH 7.4) containing 1% DMSO. λ_{ex} = 475 nm and slit width of 11 nm × 9 nm.

dye NBD-SO had high specificity towards Cys/Hcy (Fig. S15 in Supporting information). Moreover, the reaction mechanism of nucleophilic substitution reaction was predicted by ESI mass spectrometry (Fig. S16 in Supporting information).

Then, titration experiment was made to further understand the quantitative ability of dye NBD-SO responding to various concentrations of Cys/Hcy (0–8 equiv.) by UV–vis absorption spectra (Fig. S17 in Supporting information) and fluorescence spectra in Figs. 6B and C. Clearly, there was a good linear correlation between fluorescence intensity at 550 nm and the concentrations of Cys/Hcy (Fig. S18 in Supporting information). And the detection limits of dye NBD-SO were calculated to be 1.97×10^{-7} mol/L for Cys and 1.64×10^{-7} mol/L for Hcy, suggesting that it could be utilized for the determination of Cys/Hcy. Especially, the reaction kinetics of dye NBD-SO (10 μmol/L) in the presence of biothiols (100 μmol/L) showed that its response times toward Cys and Hcy were within 1 min, 15 min in Fig. 6D, respectively (Fig. S19 in Supporting information). By analyzing the fluorescence intensity and response time of all dyes, dye NBD-SO possessed good reactivity and fast response ability. Similar results of Cys/Hcy-selectivity under physiological conditions and Cys-selectivity under weakly acidic condition were also detected (Figs. S20-22 in Supporting information).

These findings described above strongly indicated that the NBD-SO dye was capable of serving as a fluorescence indicator to track the Cys and Hcy. As expected, dye NBD-SO was able to enter the cell easily and had low cytotoxicity (Fig. S23 in Supporting information). By viewing the confocal microscope images in Fig. 7, bright green fluorescence signals were detected when the non-fluorescent HeLa cells was incubated with NBD-SO (5 μmol/L) for 30 min. Combining the fact that there was no obvious fluorescence signal when NBD-SO was incubated with HeLa cells pre-treated by NEM indicated that the NBD-SO could detect endogenous biothiols. Moreover, significant fluorescence signals appearing in the NEM pre-treated HeLa cells resulted from the addition of only Cys and Hcy, respectively. These performances indicated that NBD-SO could be utilized as a tool to monitor levels of Cys/Hcy in living cells.

In conclusion, we have developed a type of fluorescent dyes based on benzo[*c*][1,2,5]oxadiazole by linking a aryl-sulphur species. Investigation on the response behavior towards amino acids indicated that they were capable of selectively detecting

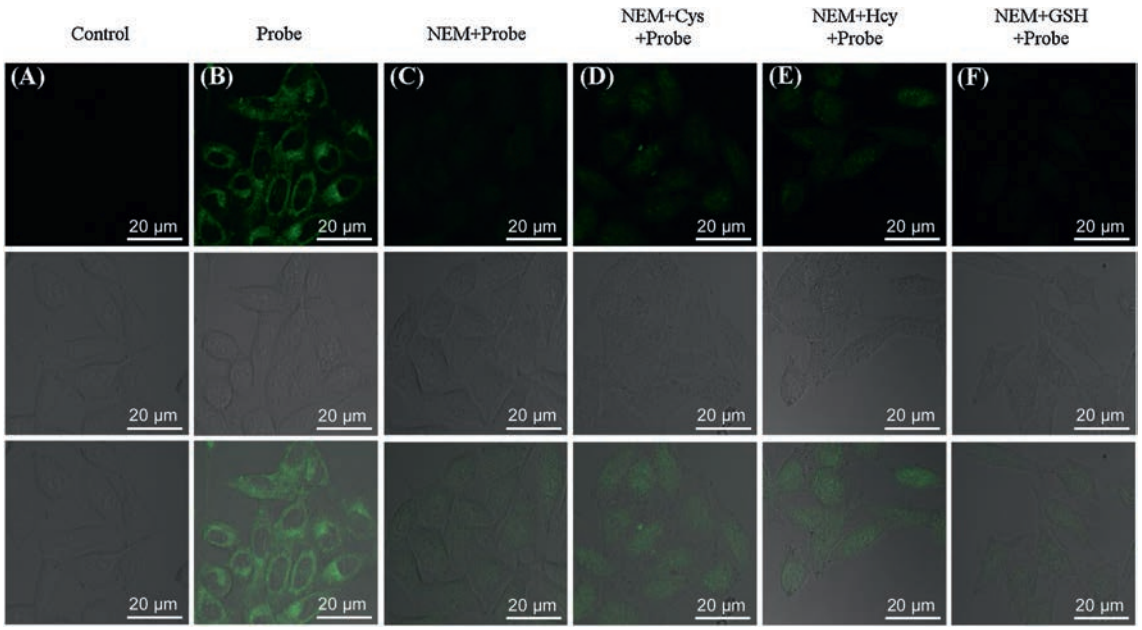

Fig. 7. Confocal microscope images of dye NBD-SO responding to biothiols in HeLa cells. (A) Fluorescence images of HeLa cells as control. (B) Fluorescence images of HeLa cells incubated with dye NBD-SO (5 μmol/L) for 30 min. (C) Fluorescence images of HeLa cells pre-treated with NEM (1 mmol/L) for 30 min, and incubated with NBD-SO (5 μmol/L) for 30 min. (D-F) Fluorescence images of HeLa cells pre-treated with NEM (1 mmol/L, 30 min), then treated with Cys (D), Hcy (E) or GSH (F) (100 μmol/L, 30 min), and then incubated with dye NBD-SO (5 μmol/L, 30 min). (Top) Images of green channel. (Middle) Images of bright field. (Bottom) Overlay of bright field and green channel.

Cys/Hcy over other amino acids containing glutathione. Interestingly, the sulphur-oxidizing dyes sulphone and sulfoxide exhibited a faster response time for Cys/Hcy. Especially, the sulfoxide dye presented a better reactivity and membrane penetrability compared with sulphone-based benzo[*c*][1,2,5]oxadiazole dye, and was able to track the Cys/Hcy in living cells. Our work provides an efficient strategy to change the responsive performance of fluorescent dyes through a simple oxidation approach. We believe it will be able to be applied in the design of fine fluorescent dyes in future.

Declaration of competing interest

We further confirm that the authors declare no competing interest.

Acknowledgments

This work was supported by the National Natural Science Foundation of China (Nos. 21676113, 21402057, 21772054, 21472059), Distinguished Young Scholar of Hubei Province (No. 2018CFA079), Youth Chen-Guang Project of Wuhan (No. 2016070204010098), the 111 Project B17019, the Ministry-Province Jointly Constructed Base for State Key Lab-Shenzhen Key Laboratory of Chemical Biology (Shenzhen), the State Key Laboratory of Materials-Oriented Chemical Engineering (No. KL17-10), Open Project Fund of Key Laboratory of Natural Resources of Changbai Mountain & Functional Molecules (Yanbian University), Ministry of Education (No. NRFM201701), the Foundation of Key Laboratory of Synthetic and Biological Colloids, Ministry of Education, Jiangnan University (No. JDSJ2017-07), the Self-determined Research Funds of CCNU from the Colleges' Basic Research and Operation of MOE (No. CCNU18TS012). We thank Professor Xin Zhou and Miss Yuanzhi Shen for their great help.

Appendix A. Supplementary data

Supplementary material related to this article can be found, in the online version, at doi:https://doi.org/10.1016/j.cclet.2020.02.047.

References

[1] (a) S.Y. Zhang, C.N. Ong, H.M. Shen, Cancer Lett. 208 (2004) 143–153;
(b) Z.A. Wood, E. Schröder, J.R. Harris, L.B. Poole, Trends Biochem. Sci. 28 (2003) 32–40.
[2] (a) S. Shahrokhian, Anal. Chem. 73 (2001) 5972–5978;
(b) T.P. Dalton, H.G. Shertzer, A. Puga, Annu. Rev. Pharmacol. Toxicol. 39 (1999) 67–101.
[3] (a) Y.K. Yue, F.J. Huo, F.Q. Cheng, et al., Chem. Soc. Rev. 48 (2019) 4155–4177;
(b) Z.Q. Guo, Y.G. Ma, Y.J. Liu, et al., Sci. China Chem. 61 (2018) 1293–1300;
(c) L.J. Tang, M.G. Tian, H.B. Chen, et al., Dyes Pigm. 158 (2018) 482–489;
(d) P. Ning, W.J. Wang, M. Chen, Y. Feng, X.M. Meng, Chin. Chem. Lett. 28 (2017) 1943–1951.
[4] (a) H. Zhang, K. Li, L.L. Li, et al., Chin. Chem. Lett. 30 (2019) 1063–1066;
(b) Y.K. Yue, F.J. Huo, X.Q. Li, et al., Org. Lett. 19 (2017) 82–85;
(c) F.J. Huo, Y.Q. Sun, J. Su, et al., Org. Lett. 11 (2009) 4918–4921;
(d) Y.F. Kang, L.Y. Niu, Q.Z. Yang, Chin. Chem. Lett. 30 (2019) 1791–1798;
(e) L. Yang, H.Q. Xiong, Y.N. Su, et al., Chin. Chem. Lett. 30 (2019) 563–565;
(f) Y. Yang, H. Wang, Y.L. Wei, J. Zhou, et al., Chin. Chem. Lett. 28 (2017) 2023–2026;
(g) M.Y. Li, P.C. Cui, K. Li, et al., Chin. Chem. Lett. 29 (2018) 992–994;
(h) S. Lee, J. Li, X. Zhou, J. Yin, J. Yoon, Coord. Chem. Rev. 366 (2018) 29–68;
(i) J.C. Xu, H.Q. Yuan, L.T. Zeng, G.M. Bao, Chin. Chem. Lett. 29 (2018) 1456–1464;
(j) C.X. Yin, K.M. Xiong, F.J. Huo, J.C. Salamanca, R.M. Strongin, Angew. Chem. Int. Ed. 56 (2017) 13188–13198;
(k) L.Y. Niu, Y.Z. Chen, H.R. Zheng, et al., Chem. Soc. Rev. 44 (2015) 6143–6160.
[5] (a) L.Y. Niu, Y.S. Guan, Y.Z. Chen, et al., J. Am. Chem. Soc. 134 (2012) 18928–18931;
(b) J. Liu, Y.Q. Sun, Y.Y. Huo, et al., J. Am. Chem. Soc. 136 (2014) 574–577;
(c) Y.K. Yue, F.J. Huo, P. Ning, et al., J. Am. Chem. Soc. 139 (2017) 3181–3185;
(d) K. Umezawa, M. Yoshida, M. Kamiya, T. Yamasoba, Y. Urano, Nat. Chem. 9 (2017) 279–286;
(e) H.H. Song, Y.M. Zhou, H.N. Qu, et al., Ind. Eng. Chem. Res. 57 (2018) 15216–15223;
(f) S.Y. Lim, K.H. Hong, D.I. Kim, H. Kwon, H.J. Kim, J. Am. Chem. Soc. 136 (2014) 7018–7025;
(g) J. Yin, Y. Kwon, D. Kim, et al., J. Am. Chem. Soc. 136 (2014) 5351–5358;
(h) M.H. Lee, J.H. Han, P.S. Kwon, et al., J. Am. Chem. Soc. 134 (2012) 1316–1322;
(i) G.X. Yin, T.T. Niu, T. Yu, et al., Angew. Chem. Int. Ed. 58 (2019) 4557–4561;
(j) B. Tang, Y.L. Xing, P. Li, et al., J. Am. Chem. Soc. 129 (2007) 11666–11667;
(k) T.B. Ren, Q.L. Zhang, D.D. Su, et al., Chem. Sci. 9 (2018) 5461–5466;
(l) L.W. He, X.L. Yang, K.X. Xu, X.Q. Kong, W.Y. Lin, Chem. Sci. 8 (2017) 6257–6265.
[6] (a) Z.Q. Xu, X.T. Huang, M.X. Zhang, et al., Anal. Chem. 91 (2019) 11343–11348;
(b) Z.Q. Xu, M.X. Zhang, G.J. Li, et al., Dyes Pigm. 171 (2019)107685;
(c) X. Han, Y.H. Liu, G.T. Liu, et al., Chem. Asian J. 14 (2019) 890–895;
(d) Z.Q. Xu, X.T. Huang, X. Han, et al., Chem 7 (2018) 1609–1628;
(e) G. Liu, X. Han, J. Zhang, et al., Dyes Pigm. 148 (2018) 292–297;
(f) G.T. Liu, W.J. Chen, Z.Q. Xu, Org. Biomol. Chem. 16 (2018) 5517–5523;
(g) M.J. Cao, H.Y. Chen, D. Chen, et al., Chem. Commun. 52 (2016) 721–724.
[7] (a) J. Liu, Y.Q. Sun, H.X. Zhang, et al., Chem. Sci. 5 (2014) 3183–3188;
(b) D.H. Ma, D. Kim, E. Seo, S.J. Lee, K.H. Ahn, Analyst 140 (2015) 422–427;
(c) F.Y. Wang, L. Zhou, C.C. Zhao, et al., Chem. Sci. 6 (2015) 2584–2589;
(d) L. Song, Q. Sun, N. Wang, et al., Anal. Methods 7 (2015) 10371–10375;
(e) D. Lee, G. Kim, J. Yin, J. Yoon, Chem. Commun. 51 (2015) 6518–6520;
(f) C.Y. Zhang, S. Wu, Z. Xi, L. Yi, Tetrahedron 73 (2017) 6651–6656;
(g) D. Lee, K. Jeong, X. Luo, et al., J. Mater. Chem. B 6 (2018) 2541–2546;
(h) S.G. Wang, H.H. Yin, Y. Huang, X.M. Guan, Anal. Chem. 90 (2018) 8170–8177;
(i) J.M. Wang, L.Q. Niu, J. Huang, et al., Dyes Pigm. 158 (2018) 151–156;
(j) J.H. Gao, Y.F. Tao, J. Zhang, et al., Chem. Eur. J. 25 (2019) 11246–11256.
[8] (a) X.L. Sheng, D. Chen, M.J. Cao, et al., Chin. J. Chem. 34 (2016) 594–598;
(b) Z.Q. Xu, M.X. Zhang, Y. Xu, et al., Sens. Actuators B 290 (2019) 676–683.
[9] Y.J. Jiang, J. Cheng, C.Y. Yang, et al., Chem. Sci. 8 (2017) 8012–8018.
[10] L.Y. Niu, H.R. Zheng, Y.Z. Chen, et al., Analyst 139 (2014) 1389–1395.
[11] B.C. Zhu, M. Zhang, L. Wu, et al., Sens. Actuators B 257 (2018) 436–441.